STAR Note 424
Calibration of the STAR Forward Time Projection Chamber with Krypton-83m

Tobias Eggert
Max-Planck-Institut für Physik, München, Germany

July 31, 2000

Abstract

The principles of the calibration of a time projection chamber with radioactive Krypton-83 are explained. The properties and advantages of ^{83}Kr are summarized and compared to other radioactive calibration sources. It was shown that the Krypton calibration for the STAR FTPC is feasible and recommendable although the pad geometry of the FTPC causes a considerable deterioration of the measured spectrum due to partially detected charge clusters.

1 The STAR Forward TPC

The high track density in the forward and backward region of the STAR experiment ($2.5 < |\eta| < 4$) required a special design for the tracking detectors in these regions. In contrast to conventional time projection chambers (TPCs), the two Forward TPCs of the STAR detector use radial drift fields, and the curved multi-wire proportional chambers (readout chambers) are part of the outer cylinder walls. This provides very good position resolution and two-track separation. In order to minimize the number of readout channels the surface is covered only partially by cathode pads. There are 10 padrows per FTPC, with 960 pads each. The length of one pad is 20 mm (in z direction, where z points along the beam pipe) and the pad pitch is 1.9 mm (in azimuthal direction ϕ). For further details on the STAR FTPC, see [1, 2].

As the padrows are not adjacent[1] to each other, a problem arises when localized charge clusters from radioactive decays are to be detected. As illustrated in figure 1, only a fraction of the cluster charge can be collected by the pads when the cluster is located at the border of a padrow. The question whether a calibration with a radioactive source can nevertheless be done triggered a systematic investigation on the practicability of a calibration with radioactive Krypton.

2 The Calibration

A calibration is needed to compensate front-end electronics (FEE) and gas gain variations. The gain of the pre-amplifier electronics varies from chip to chip and within

[1] The distance between the padrows is 65 mm.

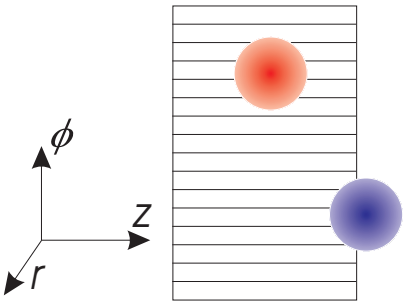

Figure 1: Two electron clusters produced by Krypton decays. As the padrows are not adjacent to each other, for some of the clusters the charge can only be partially detected.

a chip from channel to channel. Moreover, variations in gas gain may occur due to geometrical non-uniformities and inhomogeneous electric fields.

A straightforward and effortless calibration can be perfomed by injecting calibrated charge pulses into the anode wires of the readout chambers. This induces a charge on each pad, where the measured charge q (i. e. integrated ADC channels) is proportional to the channel's gain. Multiplicative calibration constants are obtained by dividing the average charge of all pads by the induced charge on a single pad.

However, pulsing the anode wires induces a signal on all pads simultaneously producing a large current load on each FEE channel which may result in a modification of the electronics response. Thus, the pulser calibration can only be considered as a first step in the calibration procedure.

Although particle identification via $\mathrm{d}E/\mathrm{d}x$ measurement is difficult [2, Sect. 6.6] with the STAR FTPC, an energy calibration is useful to optimize the position measurement accuracy. It can easily be done with a radioactive source such as ^{83}Kr which is injected into the chamber gas. As the decay energies are known, the corresponding energies can be assigned to the peaks of the charge spectra. However, because of the high decay energies of ^{83}Kr, the anode voltage U has to be reduced from the value suitable for mimimally ionizing particles. The results from the energy calibration must then be extrapolated to higher gain voltages. As the dependence of the amplification on the anode voltage has been measured[2], such an extrapolation is still very precise.

Further applications of the calibration using ^{83}Kr are a cross-check of the pulser calibration, and an investigation of gas flow effects in the chamber by studying the location of Krypton decays at the beginning of the injection. Moreover, a calibration is needed to check the detector linearity over a wide energy range, and to monitor the long term detector stability.

The calibration method using Krypton-83 has been developed by the ALEPH collaboration [3] and is being used by the NA 49 experiment very succesfully were the achieved precision is better than 0.5 % [4].

3 Properties of Krypton-83

^{83}Kr is a very useful isotope for calibrating a time projection chamber for several reasons: in contrast to other frequently used calibration sources such as ^{55}Fe, ^{83}Kr is a gas which can be distributed over the chamber volume using the existing gas

[2] The amplification factor is approximately doubled when the anode voltage is increased by 100 V

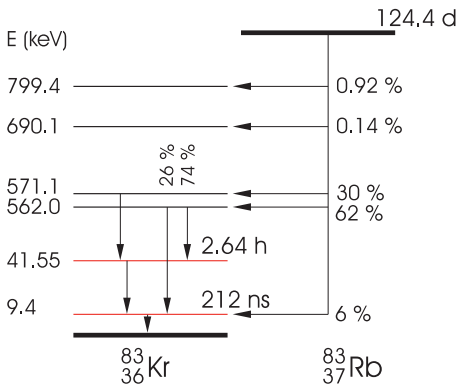

Figure 2: Decay scheme of ^{83}Rb $\rightarrow$ ^{83}Kr. The ground state of ^{83}Rb decays to the isomeric excited state ^{83m}Kr. The most important levels of ^{83}Kr for calibration are the 41.55 keV level which is populated through the intermediate 571 keV and 562 keV levels, and the 9.4 keV state which is populated from both the decay of ^{83}Rb directly as well as fed down from higher levels.

system. Therefore, no laborious unmounting of the chamber and installation of Fe strips is necessary. The short life-time ($\tau = 2.6$ h) of the isomeric state ^{83m}Kr ensures that the chamber operates normally once a few half-lives have passed after cutting off the Krypton supply to the chamber. If required, the gas can be left within the closed gas system until the radioactivity subsides. Krypton's parent isotope ^{83}Rb has a sufficiently long life-time ($\tau = 124$ d), is a solid, and thus may be placed into the gas stream via a bypass line.

As it is not possible to trigger on the Krypton decays, a random trigger must be used. The decay rate must be high enough to ensure good statistics within a reasonable time (an estimate of the number of events needed is done at the end of section 4). Due to random triggering there is no information on the decay position in the drift direction. Therefore, to obtain a clean spectrum, absorption (mainly caused by oxygen pollution in the gas) must be small (0.8 % of the electrons are absorbed per μs drift time at an oxygen concentration of 10 ppm).

^{83}Kr is a stable isotope produced from ^{83}Rb which decays by electron capture with a life-time of 124 days. The decay scheme is shown in figure 2. The ground state of ^{83}Kr is not populated directly in the decay of ^{83}Rb but via transitions from intermediate levels. The most important levels of ^{83}Kr for drift chamber calibration are the isomeric 41.55 keV state ^{83m}Kr ($\tau = 2.64$ h) and the 9.4 keV level ($\tau = 212$ ns). The isomeric state decays entirely by an E3 transition to the 9.4 keV level. In contrast to other common calibration sources like ^{55}Fe or ^{57}Co, almost no low energy photons are produced and the transition proceeds almost entirely by internal conversion ($e^-/\gamma \approx 2 \cdot 10^3$).

The resulting decay spectrum is shown in figure 3. The strong peak at 41.6 keV is due to the decay of the 41.6 keV isomeric state via the 9.4 keV state. The total energy in this cascading decay is collected in one charge cluster because of the short life-time of the 9.4 keV state. A smaller 32.2 keV peak is due to the escape of the 9.4 keV photon. The peak at 9.4 keV results from either the conversion of the 9.4 keV γ or the summed 9.4 keV electron energy separated from the 32.2 keV transition which preceeds it. In addition, K, L, M, and N shell electrons are emitted in the IC process, and the subsequent de-excitation of the electron holes produces either X-rays or Auger electrons. This results in further peaks at 12.7 keV, 19.5 keV, 27.5 keV, and 28.9 keV. For a detailed description and explanation of the released Auger electron and γ-energies, see [5].

Figure 4 shows a more detailed simulation where partially detected clusters caused

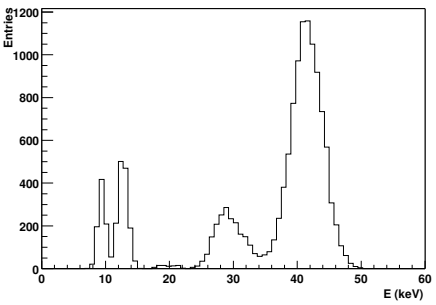

Figure 3: Simulated decay spectrum of ^{83m}Kr with an assumed line width of 6 %. Noise is not included.

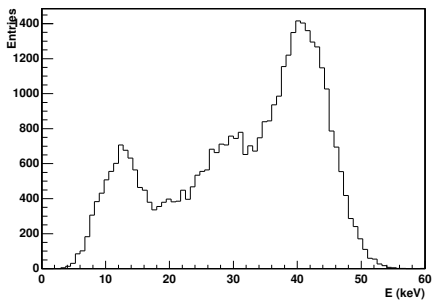

Figure 4: Simulation of the ^{83m}Kr decay spectrum as seen by the two padrows of the test-setup. Diffusion, partially detected clusters, and a threshold cut are taken into account.

by the pad geometry, diffusion, the detector resolution, and cut criteria comparable to those in the experiment were considered. The 41.6 keV peak is clearly visible while the 9.4 keV and the 12.6 keV peak are hardly separable. Besides, the shape of the low energy part of the spectrum is strongly affected by the chosen threshold.

4 The Measurements

As neither the STAR FTPC nor the FTPC readout electronics were completed when the measurements were performed, a small test-setup using the NA 49 readout electronics [6, 7] was constructed. For this test-setup, the same materials, gas-mixture, and a pad geometry comparable to the FTPC (two non-adjacent padrows with 16 pads each) were used. The major differences between the test-setup and the FTPC was the axial drift field (in contrast to the radial drift field of the FTPC) and the planar readout chamber. However, the charge deposited on the pads is hardly affected by the drift field geometry and the cluster sizes were comparable to those measured in the radial test TPC.

The calibration was performed in three steps: the pulser calibration, the calibration with ^{55}Fe, and the calibration with ^{83m}Kr.

4.1 The Preparatory Calibrations

The pulser calibration was described earlier in section 2. Each preamlifier/shaper chip shows a characteristic drop in amplification with increasing channel number. The amplification factors differ by up to 15 %. This behavior is a property of the architecture of the NA 49 FEE chips and is not observed in the FTPC electronics were the fluctuations of the amplification gain is below 3 %. Thus, a pad-wise calibration was nessecary for the test-setup but might not be needed for the calibration of the FTPC. However, the pulse shape of the FTPC electronics is affected as the current load on the chip changes. The rise time of the pulse is reduced as the number of pulsed channels increases [8] which will affect the total integrated cluster charge. Thus, a cross-check of the pulser calibration has to be performed.

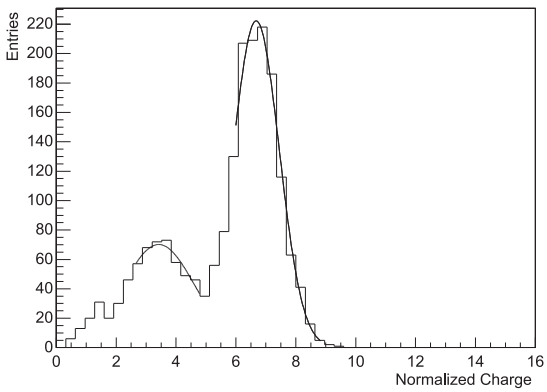

Figure 5: A measured Fe spectrum on a single pad. In these measurement the charge was normalized in such a way that the average normalized charge of all pads corresponds to the decay energy in keV. A combined fit consisting of two Gaussians was performed and the two separate Gaussians are shown in this plot.

For the measurements with the ^{55}Fe source, two Aluminium strips incorporated with ^{55}Fe were mounted at the drift field cage cathode plate opposite to the two padrows. ^{55}Fe decays via electron capture to ^{55}Mn which subsequently emits a γ with an energy of 6 keV. This γ may ionize an Argon atom in the gas which releases an electron from the K-shell. In addition, either Auger electrons or an escaping γ are emitted, the latter being responsible for the 3 keV escape peak. The supplementary calibration using ^{55}Fe was performed for several reasons:

- A cross-check of the pulser calibration and a first order energy calibration was needed to tune the anode voltage for the Krypton measurements.
- Determining the width of the 6 keV main peak and the 3 keV escape peak gave an accurate measurement of the chamber resolution.
- A comparison of the gas amplification at anode voltages in the operating range of the FTPC (1,700 V to 1,800 V) was required.
- The clear Fe spectrum allowed a straightforward determination of suitable cut criteria in order to reduce noise.

As the electron energy deposition of ^{55}Fe corresponds to the energy deposition of minimally ionizing and heavier particles produced in RHIC collisions, an energy calibration at the FTPC's operating anode voltage of $U = 1{,}750$ V was performed. In addition, further measurements at voltages from 1,700 V to 1,800 V were carried out. These results were extrapolated to lower voltages in order to find the anode voltage where the complete Kr spectrum can be detected without electronics saturation caused by the high energy decays.

For each pad a separate Fe spectrum was measured and a combined fit of the two peaks was performed (see figure 5). For the calculation of the calibration factors only the position of the 6 keV peak was considered. The width of the peak and hence the detector resolution were determined to be $\approx 12\,\%$. The positions of the fitted Gaussians on the charge spectra of each pad (except the marginal pads) is shown in figure 6. By applying the Fe calibration factors from a reference measurement at 1,750 V to measurements at different anode voltages, the consistency of the Fe calibration and

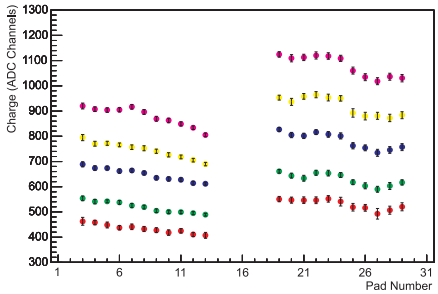

Figure 6: The measured charge q (integrated ADC channels) from the 6 keV Fe decays of each pad without any calibration. Anode voltages from the bottom up: U = 1,700 V, 1,725 V, 1,750 V, 1,775 V, 1,800 V.

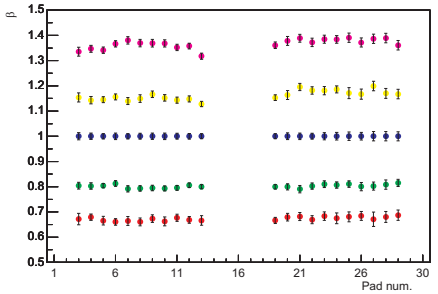

Figure 7: The measured charge from Fe decays of each pad i (as in figure 6) with calibration factors obtained by the reference measurement at an anode voltage of 1,750 V. $\beta = q_i(U)/q_i(1{,}750\,\mathrm{V})$

thus the expected precision for the Kr calibration was investigated (see figure 7). The resulting uncertainty is estimated to be $< 2\,\%$.

The comparison of the calibration factors obtained with the pulser and the iron source shows notable differences. The drop in amplification with increasing channel number in the latter is smaller because only a few pads receive charge signals in the case of the Fe mesaurement.

A thorough investigation of cut criteria showed that constraints on the cluster size in r and ϕ direction significantly improve the spectra and reduce noise and background. An effective background rejection is of great importance for the following calibration with ^{83m}Kr. Moreover, clusters located at the marginal pads of each padrow were rejected.

4.2 The Krypton Calibration

In a first step, Kr spectra were recorded at high anode voltages (1,600 V and 1,700 V), focusing on the 9 keV peak. The calibration factors from the Fe reference measurement were applied to the data and the spectra from the single pads were combined to one spectrum. By this means, the accuracy of the extrapolation of the gas gain measurements with Fe from high anode voltages to lower voltages could be checked. This extrapolation was correct within an error $< 1\,\%$. The optimum anode voltage for collecting the complete Kr spectrum was determined to be 1,500 V.

In the second step, a high statistics run at 1,500 V was carried out in order to allow a pad-wise calibration with the 41.6 keV peak. In some of the high energy decays, several electrons are produced consecutively in a short time span. This results in charge clusters with multiple peaks. As the summed electron energy is relevant, a special cluster finder[3] was used that does not deconvolute overlapping clusters, but sums up the total charge.

The cuts determined by the Fe measurements were applied and the calibration constants were then obtained by fitting a simple Gaussian to the upper part of each

[3]The cluster finder calculates the charge and other parameters like position and width of each found cluster from the raw data.

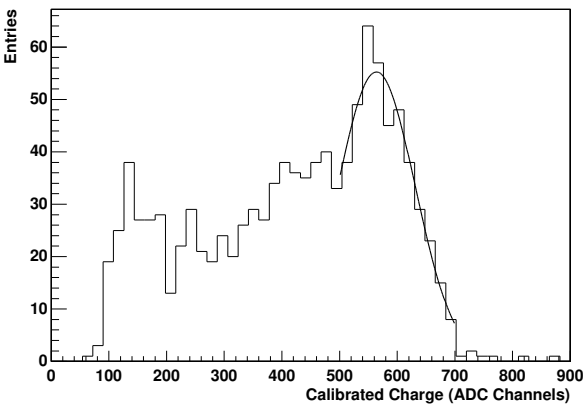

Figure 8: Krypton spectrum of a single pad at an anode voltage of 1,500 V. At higher anode voltages, only the low energy part of the spectrum could be detected.

spectrum (see figure 8). This calibration was repeated iteratively several times since the cluster charge of several pads with different calibration factors is summed up although the resultig charge is assigned to the spectrum of the central pad.

Finally, a total Kr spectrum was obtained by combining the calibrated spectra of the single pads (except the marginal pads). This measured Kr spectrum is in very good agreement with the simulation (compare figures 4 and 9). The position of the peaks could be determined by a combined fit to a satisfactory precision. Both the linearity and the accuracy of the fitting procedure were checked by normalizing all fitted peaks to the high energy peak at 41.6 keV. The deviations from the expected positions were below 5 %.

The gas pressure, temperature, and drift velocity were not monitored during the measurements. As the gas amplification is relatively sensitive to these values, a more precise calibration can be attained when appropriate correction factors are applied to the data.

In order to obtain a spectrum where the 41.6 keV peak can be fitted precisely, at least 1,000 decay events that fulfill the cut criteria are required. With moderate cut criteria, 80 % of the events pass the cuts and thus 1,250 events have to be recorded. Consequently, if a pad-wise calibration of the FTPC's 19,200 pads is required, a total of $24 \cdot 10^6$ events is needed. For a chip-wise calibration (each chip reads out 16 pads) this number decreases to $1.5 \cdot 10^6$ events. Assuming that the data can be written with a rate of 15 Hz and that there is one Kr decay detected per trigger, it takes about 28 hours to record $1.5 \cdot 10^6$ events.

5 Conclusions

It was shown that a calibration with Krypton-83m is a very useful and convenient calibration method for the STAR FTPC. Its practicability is not affected by the FTPC's pad geometry. With this method, both a compensation of deviations in amplification and a precise energy calibration can be obtained.

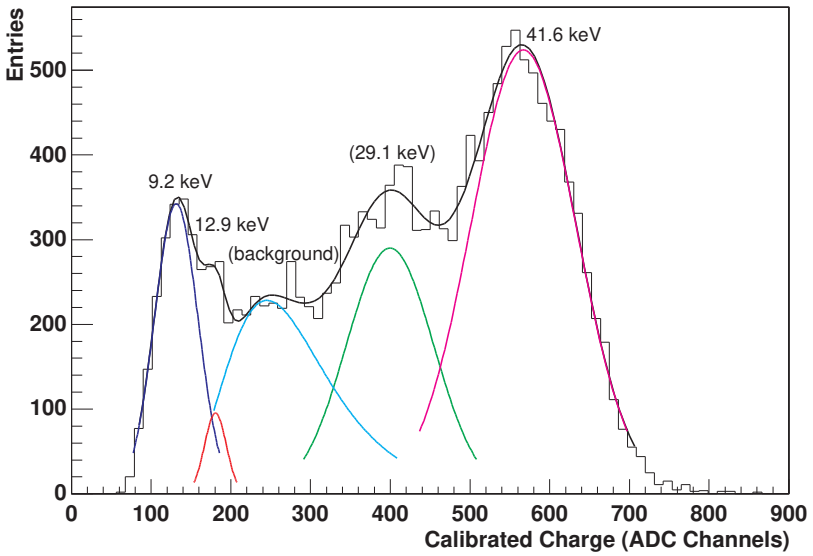

Figure 9: The measured Kr spectrum of all pads calibrated with the calibration constants obtained from the Krypton spectra of the single pads. A combined fit using 4 Gaussians (for the peaks) and one Landau distriution (for the background) was performed. The maximum of the high energy peak was assigned an energy of 41.6 keV and thus the energy of the other peaks was calculated.

References

[1] A. Schüttauf and the STAR Collaboration, A Forward TPC for STAR, Nuclear Physics A661 (1999) 677c–680c, 1999

[2] The STAR FTPC Collaboration, Proposal for the Forward Time Projection Chamber for the STAR Detector, MPI PhE/98 3, 1998

[3] D. Decamp et al., Nuclear Instruments and Methods in Physics Research A 294 (1990) 121, 1990

[4] S. Afanasiev et al., The NA 49 Large Acceptance Hadron Detector, Nuclear Instruments and Methods in Physics Research A 430 (1999) 210–244, 1999

[5] B. Lasiuk, C. A. Whitten, Use of Krypton-83 as a Calibration Source for the STAR TPC, STAR Note 360, 1998

[6] W. Rauch, The NA 49 Data Acquisition System, CERN RT39-52, 1993

[7] F. Bieser et al., Design and Performance of TPC Readout Electronics for the NA 49 experiment, Nuclear Instruments and Methods in Physics Research A 385 (1997) 535–546, 1997

[8] B. Lasiuk, Investigation of the STAR FEE Response to the FEE Pulser at the TPC System Test, STAR Note 324, 1998